Eur. Phys. J. D **38**, 495–500 (2006)
DOI: 10.1140/epjd/e2006-00036-0

THE EUROPEAN PHYSICAL JOURNAL D

Modelling electron-N_2 scattering in the resonant region

Integral cross-sections from space-fixed coupled channel calculations

S. Telega[a] and F.A. Gianturco[b]

Department of Chemistry, University of Rome "La Sapienza", Piazzale A. Moro 5, 00185, Roma, Italy

Received 11 November 2005
Published online 21 February 2006 – © EDP Sciences, Società Italiana di Fisica, Springer-Verlag 2006

Abstract. Quantum calculations of the resonant vibrational excitation of N_2 by electron impact are carried out using a model potential for exchange and correlation-polarization forces and exact static interaction. The inelastic process is treated within a coupled channel, space-frame formulation and final cross-sections are tested for convergence within less than 0.01% of their values. Comparison with the experiments yields very good agreement with the latter data in the resonance region and suggests possible extension to calculations near the threshold openings for rovibrational inelastic processes induced by electron impact.

PACS. 34.80.Bm Elastic scattering of electrons by atoms and molecules – 34.80.-i Electron scattering

1 Introduction

The study of the quantum dynamics involved in the scattering of low-energy electrons from molecular gases is now a very mature subject in which a great deal of data, both experimentally and theoretically, have been gathered over the years and have dealt with a very broad range of molecular systems [1,2]. The object of several of such studies has been to unravel as much as possible the details of the energy transfer processes at the molecular level and to provide a correspondingly detailed theoretical explanation of the features brought to light by the increased resolution of the state-of-the-art experiments [3].

The computational rendition of the theoretical quantum description of these inelastic collisions has to always balance the demands for a realistic treatment of the processes and the increased complexity of the calculations involved. Thus, it is always useful to be able to develop model treatments which are accurate and realistic when it comes to reproducing the scattering attributes that they can yield, but which can also keep within reasonable limits the corresponding computational effort [4].

A case in point is provided by the correct description of rotovibrational excitations in simple molecular gases by a single collision with a low-energy electron at energies close to the openings of such channel thresholds. The usual theoretical treatment involves solving the rotovibrational inelastic problem in the Body-Fixed (BF) reference frame and carrying out vibrational coupled-channel (CC) calculations in the same molecular reference frame that can take the advantage of the point-group symmetries of the target vibrations [5]. On the other hand, when the collision energies go down to a few meV above thresholds, or in the vicinity of resonances, the interaction times between the impinging electron and the rotating molecule become larger, so that the recoupling of the orbital and rotational angular momenta requires using the external, laboratory frame as a reference space: the Space-Fixed (SF) representation [6]. In such instances, therefore, the calculations not only require the inclusion of several rotational channels which are asymptotically closed [4] but further require the expansion over a large number of vibrational channels since they are meant to correctly describe the marked distortion of the target molecular structure that occurs upon attachment of the impinging electron, especially at energies where narrow resonances exist [5].

In the present work we therefore intend to focus on that very region and to develop a model potential that is able to produce in local form the full $e^- - N_2$ interaction potential over a broad range of molecular geometries. Such model will be tested around the well-known Π_g resonance of N_2^- [7], in order to assess its capabilities for reproducing such well-known experimental features [8].

The following Section 2 therefore describes our method while Section 3 reports calculations performed around the Π_g resonance region. Section 4 summarizes our conclusions.

2 Theoretical formulation

2.1 The quantum dynamics

In order to ultimately describe the structural distortions that are induced into the target molecule by the impinging

[a] *Permanent address:* Faculty of Applied Physics and Mathematics, Gdansk University of Technology, ul. Narutowicza 11/12, Gdansk, Poland.
[b] e-mail: `fagiant@caspur.it`

particle, the total scattering wavefunction can be expanded in terms of asymptotic rotational and vibrational eigenfunctions of the isolated partner

$$\mathcal{H}_{mol}(\mathbf{R})\chi_\nu(R)Y_{jmj}(\hat{\mathbf{R}}) = \left[\varepsilon_\nu + \frac{\hbar^2}{2I}j(j+1)\right]\chi_\nu(R)Y_{jmj}(\hat{\mathbf{R}}) \quad (1)$$

where ε_ν is the vibrational eigenvalue, I the molecular moment of inertia [6] ($\hat{R}$) gives the space orientation of the molecular bond and $\mathbf{R}$ the internuclear separation. Hence, the total scattering wavefunction is given as

$$\Psi_n(E,\mathbf{r}_e,\mathbf{R}) = \sum_f u_{i\to f}(\mathbf{r}_e,E)\chi_f(R)\,Y_f(\hat{\mathbf{R}}) \quad (2)$$

where $|f\rangle$ denotes the final states of the vibrating molecule that are involved in the expansion and the $u_{i\to f}(\mathbf{r}_e,E)$ are the channel components of the scattering wavefunction which have to be determined by solving the usual Schrödinger equation subject to its scattering boundary conditions, with $\mathbf{r}_e$ being the scattered electron vector position from the molecular center of mass

$$u_{i\to f}(\mathbf{r}_e) \to \delta_{if}h^{(-)}(\mathbf{r}_e) - S_{if}h^{(+)}(\mathbf{r}_e) \text{ as } (\mathbf{r}_e)\sim\infty \quad (3)$$

where $h^{(\pm)}(\mathbf{r}_e)$ is a pair of linearly independent free partial solutions defined as

$$h_{if}^{(\pm)} \sim \delta_{if}k_i^{-1/2}\exp\left[i(k_ir \pm l_i\pi/2)\right]. \quad (4)$$

When they are chosen to be appropriate Riccati-Hankel functions, then the S_{if} coefficients become the elements of the reduced scattering matrix, often additionally labelled by the total angular momentum of the system: $\mathbf{J}=\mathbf{j}+\mathbf{l}$, the latter $\mathbf{l}$ being the continuum electron partial wave component. The $u_{i\to f}$ are expanded in products of total angular momentum eigenfunctions and of radial functions $\varphi^J_{\lambda\lambda'}(E,r_e)$, where J is the magnitude of the total angular momentum and, $\lambda'=(j',l')$. The radial functions are in turn solutions of the familiar set of coupled, second order homogeneous differential equations (in the case of local interactions) [9,10] which represent the Coupled Channel formulation

$$\left[\frac{d^2}{dr_e^2}\mathbf{I}^2 - \frac{1}{r_e^2}\mathbf{l}^2 + \mathbf{K}_\nu^2\right]\mathbf{\Phi}^J_\nu(E,r_e) = \sum_{\nu'}\mathbf{U}^J_{\nu\nu'}\mathbf{\Phi}^J_{\nu'}(E,r_e) \quad (5)$$

where $\mathbf{I}$ is the unit matrix, $\mathbf{\Phi}^J$ is the matrix of radial functions and

$$(\mathbf{l}^2)_{\lambda\lambda'} = l'(l'+1)\delta_{\lambda\lambda'} \quad (6)$$

$$(\mathbf{K}^2_\nu)_{\lambda\lambda'} = k^2_{j\nu}\delta_{\lambda\lambda'} = (2/\hbar^2)(E-E_{j\nu})\delta_{\lambda\lambda'} \quad (7)$$

$$(\mathbf{U}^J_{\nu\nu'}(r_e))_{\lambda\lambda'} = \sum_L f_L(lj;l'j';J)\langle\chi_\nu|V_L(r_e)(R)|\chi_{\nu'}\rangle \quad (8)$$

where the $f_L(lj;l'j';J)$ are the Percival and Seaton coefficients [6,11] and the coupling between the asymptotic (diabatic) target rotational and vibrational states is given by the radial matrix elements of equation (8).

The number of channels to be included in the expansion for equation (5) obviously depends on the system and on the collision energy. Furthermore, for each selected collision energy it also depends on the region of interaction that is being sampled during the search for the channel eigenfunctions. In the short-range regions, which correspond to the strongest interaction, one should include all those channels which become locally open because of the attractive features of the given potential (and which would be asymptotically closed, or at least some of them). Their number could be very large in the present situations where the Coulomb interaction is the strongest over the nuclear cusp regions. On the other hand, in the weaker asymptotic region for $r_e\sim\infty$, only a few of the open channels will be needed to describe the weaker target distortion. In between these two extreme situations there is a region of interaction where the closed channels change their importance with distance and therefore could be varied in number accordingly. Just to treat such demanding interaction forces during an exact quantum dynamics, we have recently developed [10] a suitable numerical algorithm that judiciously performs the controls along the radial evaluation process and modifies the size of the relevant S-matrix. We have called it the Modified Variable Phase Approximation (MVPA) and have employed it in the present case to solve the set of coupled equations (5). The gain in the computational effort can be of about two orders of magnitude with respect to more conventional methods [12].

Typically, for numerical convergence we needed to use the full coupling from about 10^{-5} Å (the initial integration point) out to 16.0 Å, then we could gradually reduce the K-matrix size out to 400 Å. The total angular momentum values went up to $J=3$ while the target rotational basis was extended up to 36: the rotational constant of our target was taken to be 1.989581 cm^{-1}. The multipolar coefficients of the potential expansion went up to $\lambda_{max}=34$. The number of vibrational levels included in the expansion was sixteen levels up to $\nu_{max}=15$. It indicates that over the energy range of the resonant process the N_2^- molecule which is being formed is markedly different from asymptotic shape of isolated N_2. The integration over the internuclear coordinate of the coupling matrix elements of equation (8) run from $R_{min}=0.8$ Å up to $R_{max}=1.6$ Å, covering a range of 16 vibrational levels; the latters were obtained by numerical integration over the potential energy curve [13] using our own computed potential energy points. The above parameters produce convergence of the S-matrix elements of the order of about 10^{-3}–10^{-4} with respect to further extension of the CC expansion indicated above.

2.2 The electron-molecule interaction

2.2.1 The single center expansion

We employ an ab initio, parameter-free approach which starts with the target nuclei varying their relative distance

over a preselected range of values. Furthermore, the target electrons are in their ground molecular electronic state and are described using the Hartree-Fock, Self-Consistent Field (SCF) approximation via the Single-Determinant (SD) description of $N/2$ occupied Molecular Orbitals (MOs). In our implementation of the scattering equations the occupied MOs of the targets are again expanded on a set of symmetry-adapted angular functions with their corresponding radial coefficients represented on a numerical grid [14]. In this approach, any arbitrary three-dimensional function describing a given electron, either one of the N bound electrons or the scattering electron, is expanded around a single-center (SCE) usually taken to be the c.o.m. of the global $(N+1)$ electron molecular structure

$$F^{p\mu}(r,\hat{\mathbf{r}}|\mathbf{R}) = \sum_{l,h} r^{-1} f_{lh}^{p\mu}(r|\mathbf{R}) X_{lh}^{p\mu}(\hat{\mathbf{r}}). \tag{9}$$

The above SCE representation refers here to the μth element of the pth irreducible representation (IR) of the point group of the molecule at the nuclear geometry $\mathbf{R}$. The angular functions $X_{lh}^{p\mu}(\hat{\mathbf{r}})$ are symmetry adapted angular functions given by proper combination of spherical harmonics $Y_{lm}(\hat{\mathbf{r}})$

$$X_{lh}^{p\mu}(\hat{\mathbf{r}}) = \sum_{m} b_{lmh}^{p\mu} Y_{lm}(\hat{\mathbf{r}}). \tag{10}$$

The details about the computation of the $b_{lmh}^{p\mu}$ have been given by us before and will not be repeated here [12,14,15].

2.2.2 The anisotropic potential

For a target which has a closed-shell electronic structure with n_{occ} doubly occupied orbitals φ_i, its undistorted interaction with a scattering electron is given by the Exact Static+Exchange contributions

$$V_{ESE}(\mathbf{r}) = \sum_{k=1}^{2} \frac{-Z_k}{|\mathbf{r}-\mathbf{R}_k|} + \sum_{i=1}^{n_{occ}} \left(2\hat{J}_i - \hat{K}_i\right) \tag{11}$$

where $\hat{J}_i$ and $\hat{K}_i$ are the usual local static potential and the non-local exchange potential operators, respectively. The index k labels one of the two nuclei located at the coordinate $\mathbf{R}_k$ in the c.o.m., molecular frame of reference (MF).

The non-local exchange interaction has been modeled via a local Free Electron Gas form that has been used before to simplify calculations [12,17]

$$V_{ex}^{HFEGE}(\mathbf{r}_e|\mathbf{R}) = \frac{2}{\alpha} k_F(\mathbf{r}_e) \left[\frac{1}{2} + \left(\frac{1-\eta^2}{4\eta}\right) \ln\left|\frac{1+\eta}{1-\eta}\right|\right] \tag{12}$$

where:

$$k_F(\mathbf{r}_e) = [3\pi^2\rho(\mathbf{r}_e)]^{1/2};$$
$$\eta(\mathbf{r}_e) = (k^2 + 2I_f + k_F^2)^{1/2}/k_F \tag{13}$$

the parameter appearing in the above model potential is the quantity I_f, the ionization potential of the target molecule: we are therefore expected to know the I_f values over the range of internuclear distances that contribute to the vibrationally inelastic processes. However, we are not aware of any experimental information on its changes over molecular geometries, and thus decided to treat I_f as a "tuning" parameter. The "tuning" procedure consisted of calculating the cross-section in the resonance region for the vibrationally inelastic 0–1 transition using different I_f values, and choosing the one which renders the position of the first computed resonance peak in accordance with the experiments. One should note here that, although this local modeling of the exchange potential is numerically convenient for an SF treatment of the dynamics, we cannot really tell how accurately it reproduces the scattering observables near the low-energy thresholds without carrying out additional extensive calculations. Hence, in the present work we decided to employ the adjusted parameter above ($I_f = 0.44$ a.u.) to analyse the resonance region and to obtain the best agreement with the available resonant vibrationally inelastic cross-sections. The same value of the I_f parameter will then be used without further adjustment to study in our future work other processes induced by the electron impact at much lower collision energies.

Electron-molecule scattering cross-sections (integral and differential) which are computed using only the V_{ESE} potential show in general limited agreement with experimental data of elastic scattering and become even worse when dealing with resonant scattering. The reason lies in its lack of description of the target response, i.e. of the effects of long-range polarization of the bound electrons by the charged projectile and of the short-range dynamical correlation between the latter and the molecular electrons.

In order to include in the electron-molecule potential the long-range polarization terms and the short-range dynamical correlation effects, we have implemented a local energy-independent model potential, $V_{ecp}(\mathbf{r})$, discussed in our earlier work [14,15,18]. Briefly, the V_{ecp} potential contains a short-range correlation contribution, V_{corr}, which is smoothly connected to a long-range polarization contribution, V_{pol}, both terms being specific for electron projectiles. The short-range term is obtained by finding where the two radial coefficients for $l = 0$ first intersect. This has been, in fact, what we found in many cases to be the more effective choice in terms of the global smoothness of the total potential [18]. Hence, one writes down the full potential as

$$V_{ecp}(\mathbf{r}_e|R) = \begin{cases} V_{corr}(\mathbf{r}_e|R) & r_e \le r_{match} \\ V_{pol}(\mathbf{r}_e|R) + \sum_{lm} C_{lm}\, r^{-\lambda}\, Y_{lm}(\hat{\mathbf{r}}_e) & r_e > r_{match} \end{cases}. \tag{14}$$

The C_{lm} coefficients have been determined to make the potential continuous at r_{match} and the exponent λ is a function of l such that: $\lambda(l) = 6,5,6$ for $l = 0,1,2$ and $\lambda(l) = l+2$ for $l \ge 3$. The matching functions are chosen in a way in which each term added to V_{pol} after r_{match} has

the same functional form of the first term neglected in the perturbation expansion of V_{pol}. This interaction now corresponds to solving our scattering equations using Static-Exchange-Correlation-Polarization (SECP) potentials.

The polarization term contains the spherical and non-spherical parts of the diatomic dipole polarisabilities:

$$V_{pol}^{(0)}(R) = -\frac{\alpha_0(R)}{2r_e^4}; \text{ and}$$
$$V_{pol}^{(2)}(R) = -\frac{\alpha_2(R)}{2r_e^4} P_2[\cos(\hat{\mathbf{r}}_e \cdot \hat{\mathbf{R}})] \quad (15)$$

for the $N_2(R)$ calculation of α_0 and α_2 was varied over the range of internuclear distances that are relevant to the number of coupled asymptotic vibrational levels. At the equilibrium geometries our computed values were $\alpha_{xx} = 9.82a_0^3$ and $\alpha_{zz} = 14.824a_0^3$, to be compared with the experimental values [12,17] of $\alpha_{xx}^{expt} = 10.204a_0^3$ and $\alpha_{zz}^{expt} = 14.99a_0^3$. We have (somewhat arbitrarily) scaled the radial dependence of the polarisability terms computed by us to reproduce the experimental values at R_{eq}, thus constructing a realistic long-range polarisation potential over the required range of nuclear geometries to be included in the coupling integrals of equation (8).

The full SECP interaction can be rewritten using the familiar multipolar expansion in the Space-Frame (SF) reference system of its Jacobi coordinates

$$V_{SECP}(\mathbf{r}_{e'}|\mathbf{R}) = \sum_{L=0,\,even}^{L_{max}} V_L^{SECP}(r_e|R) P_L[\cos(\hat{\mathbf{r}}_e \cdot \hat{\mathbf{R}})]. \quad (16)$$

The individual multipolar coefficients were then fitted with spline functions.

3 Results

The resonant region of the $N_2 - e^-$ scattering has been studied several times, both with theory and through experiments, over the last several years. We shall just summarize here the most recent of these studies. Wong [19] has performed measurements in the 1–4 eV energy region using a crossed beam electron spectrometer. Jung et al. [20] have used an electron impact spectrometer in their beam experiments. They considered an energy range from 0.5 to 6 eV in the angular range from 15 to 105°. Sun et al. [21] have used a conventional crossed electron-molecular beam spectrometer to measure the DCS between –20 and 130° from 0.55 to 10.0 eV. Tanaka et al. [22] further employed a crossed electron beam and molecular beam scattering technique over the angular range of 20 to 130° in the energy range from 3 to 30 eV. Brennan et al. [7] have crossed a beam of N_2^- effusing from multichannel capillary array with a beam of monoenergetic electrons in the angular range from –20 to 130° at 1.5, 2.1, 3.0 and 5.0 eV. Allan [27] has studied the energy dependence of the vibrational excitation using a trochoidal electron spectrometer. Relative DCS (superpositions of 0 and 180° data) have been normalized to the results of Jung et al. [20] at 2.25 eV to obtain the integral cross-sections.

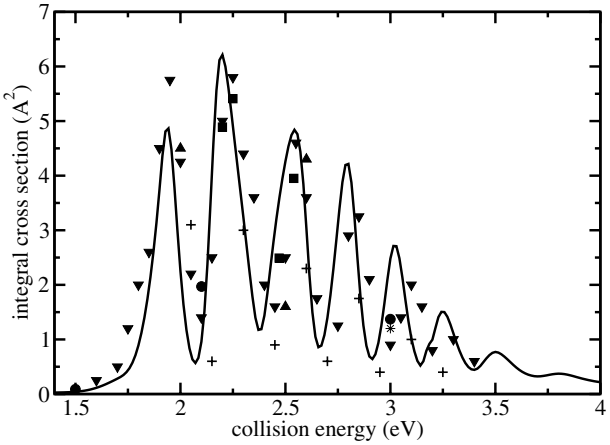

Fig. 1. Computed vibrationally inelastic cross-section for the 0−1 transition compared with the experimental data: (■) from reference [20]; (▲) from reference [21]; (∗) from reference [22]; (+) from reference [24]; (▼) from reference [19]; (●) from reference [7].

In our first Figure (Fig. 1) we present the cross-section obtained in the case of vibrational transition from the ground state to the first excited (summed over the final rotational states) compared with the selection of the existing experimental data. As it can be clearly seen, the present calculation is able to describe well the experimental phenomena in the whole resonance region. We even report for completeness the much earlier measurements by Schulz et al. The number of peaks in the oscillatory resonance structure obtained by means of the present formulation seems to indeed confirm the measurements. The extensive set of cross-section points obtained by Wong et al. [19] is followed closely by the present curve, although, from the second peak on, one may observe a certain shift towards lower energies with respect to the experimental structures. The important result of this comparison is that our approach is seen to be able to distinguish and locate all the resonance peaks predicted by the measurements. Even the old experiments of Schulz et al. [24], especially at the location of their minimum points, are well reproduced here, as our calculations render the counting of the number of their peaks possible and usable. The reported experimental points of Jung et al. [20], Sun et al. [21], Tanaka et al. [22] and Brennan et al. [7] appear on the whole to be well described by the present theoretical results, both qualitatively and quantitatively: it is an important confirmation of the validity of our chosen formalism and of our modelling of the interaction potential.

Figure 2 reports once again the 0−1 vibrationally inelastic, rotationally summed cross-section, this time in comparison with other theoretical investigations. Both of them, i.e. those of Robertson et al. [25] and R-matrix calculations by Schneider et al. [26] seem to agree with the present results in the resonance region, though one observes energy shifts in the resonance structure peaks, both towards the lower and higher energies, the most notable

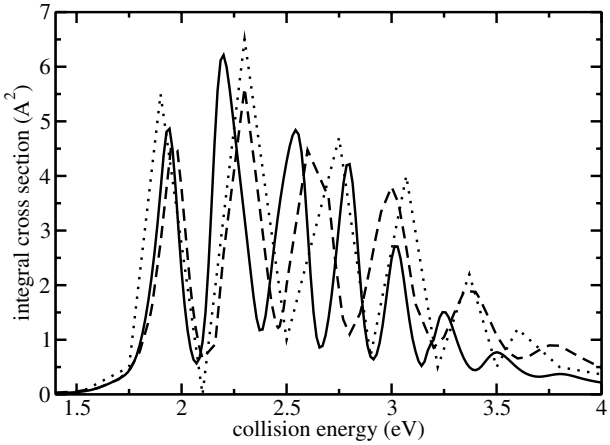

Fig. 2. Computed vibrationally inelastic cross-section for the 0–1 transition compared with the theoretical data: (——) present; (– – –) from reference [25]; (· · · · ·) from reference [26].

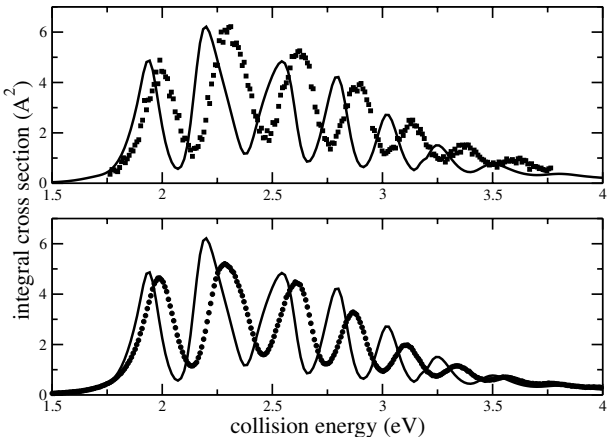

Fig. 3. Computed vibrationally inelastic cross-section for the 0–1 transition compared with the experimental: (——) present results; (■) experiments from reference [28]; (●) experiments from reference [23].

difference appearing in the energy range between 2.5 and 3.0 eV. As clearly seen, in this energy range our present calculations find two distinct peaks, the third and the forth, peaks, which are also confirmed by experimental data, while the other theoretical curves only find there one, broader peak shifted either towards lower [25] or higher [26] energies with respect to experiments. Therefore, the present results are seen to be the only ones among existing calculations which are able to yield cross-sections in agreement with the experimental findings over the broadest range of resonance energies.

Our third figure (Fig. 3) further shows the (0–1) vibrational excitation integral cross-section obtained by the present treatment and compares it with the DCS data of Allan which have produced integral cross-sections in absolute values [23]. We further compare with Buckman et al. [28], where the experimental data have been scaled, somewhat arbitrarily, so as to coincide with the measured point of Jung et al. [20] at 2.47 eV, following the technique suggested in an earlier paper of Allan [27]. Such an

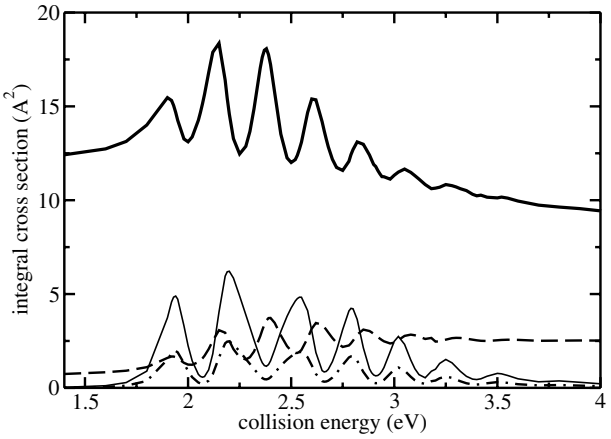

Fig. 4. Comparison between cross-sections for different processes: (▬▬) elastic; (——) vibrationally inelastic rotationally summed; (– – –) vibrationally elastic rotationally inelastic; (– · –) vibrationally inelastic rotationally elastic.

approach can be usefully employed to check the general agreement of the shape of the cross-section in question between theory and experiments. As one may see, despite the observed shift in the peaks positions, the overall structure of the resonance region is given quite closely by calculations and one can identify all the eight measured peaks, a feature which seems to confirm once again the quality of our chosen modelling of the phenomena.

The data shown by Figure 4 additionally report a comparison between the computed inelastic processes obtained for the different transitions and generated within the present formulation. As it can be observed, the total elastic cross-section is by far the biggest and appears as the dominant phenomenon in the considered energy region. The purely rotational transition ($j = 0$, $j' = 2$) is seen to be a much less efficient process, about four times less probable, although still larger than the purely vibrational excitation: the latter energy transfer is therefore much less likely to occur, especially outside the resonance region. Vibrational cross-sections, summed over the final rotational states are here much bigger than the pure rotationally inelastic ones. It indicates that, contrary to the vibrationally elastic case, rotationally inelastic transitions markedly help to enhance the probability for further vibrational excitations.

The data of Figure 5 finally present the first three contributions to the elastic cross-section, corresponding to various values of the total angular momentum: respectively 0, 1 and 2. As it may be noted, in the considered energy region, by far the biggest contribution comes from the $J = 0$ component. It provides a sort of "background" behaviour while the Π_g resonance is chiefly due to the $J = 2$ component, which is the only one to exhibit an oscillatory structure and to allow for the $l = 2$ component of the electronic angular momentum $\hat{l}$ to perform its crucial role of dynamical barrier trapping (shape resonance). Higher J components are too small to be visible in this figure.

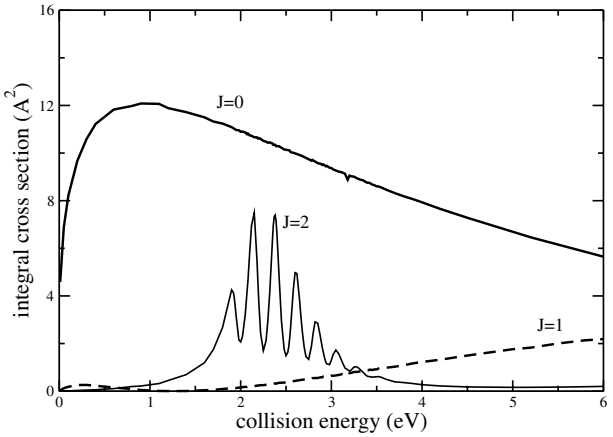

Fig. 5. Elastic cross-section: terms corresponding to the contributions from different total angular momentum values.

4 Conclusions

In the present work we have carried out the calculations concerning the ro-vibrational excitations of molecular nitrogen induced by the collisions with slow electrons in the energy range covering the well-known Π_g resonance. The overall agreement with the available data is quite satisfying, taking into account the approximations applied in order to fully exploit SF treatment of the quantum dynamics. The chosen exchange interaction model (TFEGE) seems to provide a realistic rendition of a localized interaction kernel, enabling us to perform converged electron-molecule calculations in the SF (Space Fixed) frame of reference.

In the near future we further intend to extend the calculations by applying the exchange model established in this work down to the lower energy regions, in the vicinity of the excitation thresholds for rotational and vibrational states, i.e. in the region where the BF approximations is no longer valid in describing the process and the present SF approach becomes mandatory. We hope that the SF approach, which takes into account the proper dynamics of the scattering event, will also be capable of yielding realistic results in that interesting energy range near the excitation thresholds.

The authors would like to thank Prof. Michael Allan and Prof. Steve Buckman for kindly sending us their experimental results. The discussions with Prof. Steve Buckman, Prof. Yuki Itikawa during the EPIC/EIPAM meeting in Viterbo (June, 2005) are gratefully acknowledged. The financial support of the Research Committee of the University of Rome "La Sapienza", of the CASPUR Supercomputing Center and of the EPIC EU Research Training Network n. HPRN-CT-2002-00179 are also acknowledged. One of us (S.T.) further thanks the EPIC Network for the award of a Research Fellowship at the University of Rome during the year 2004/2005.

References

1. L.G. Christophorou, J.K. Althoff, *Fundamental Electron Interactions with Plasma Processing Gases* (Kluwer Ac./ Plenum Publ., New York, 2004)
2. E.W. Mc Daniel, *Collision Phenomena in Ionized Gases* (J. Wiley and Sons Inc., New York, 1964)
3. L.G. Christophorou, J.K. Althoff, Adv. Atm. Mol. Opt. Phys. **44**, 155 (2000)
4. *Computational Methods for Electron-Molecule Collision* edited by W.M. Huo, F.A. Gianturco (Plenum Press, New York, 1995)
5. Y. Itikawa, Int. Rev. Phys. Chem. **16**, 155 (1997)
6. E.g. see: A.M. Arthurs, A. Dalgarno, Proc. Roy. Soc. A **256**, 540 (1960)
7. M.J. Brennan, D.T. Alle, P. Euripides, S.J. Buckman, M.J. Brunger, J. Phys. B **25**, 2669 (1992)
8. E.g. see: G.J. Schulz, Phys. Rev. **135**, A988 (1964)
9. F. Calogero, *Variable Phase Approach to Potential Scattering* (Academic, New York, 1967)
10. E. Bodo, R. Martinazzo, F.A. Gianturco, Comp. Phys. Comm. **151**, 187 (2003)
11. M.A. Morrison, R.W. Crompton, B.C. Saha, Z.L. Petrovic, Aust. J. Phys. **40**, 239 (1987)
12. S. Telega, F.A. Gianturco, Eur. Phys. J. D **29**, 357 (2004)
13. R.J. Le Roy, Level 7.2, Chem. Phys. Res. Report, CP-555R (2000)
14. E.g. see: F.A. Gianturco, A. Jain, Phys. Rev. **143**, 347 (1986)
15. E.g. see: R. Curik, F.A. Gianturco, J. Phys. B **35**, 1235 (2002)
16. S. Hara, J. Phys. Soc. Jpn **22**, 710 (1967)
17. S. Telega, F.A. Gianturco, Eur. Phys. J. D **36**, 251 (2005)
18. F.A. Gianturco, R.R. Lucchese, N. Sanna, J. Chem. Phys. **100**, 6464 (1994)
19. S.F. Wong: unpublished but cited in L. Dube, A. Herzenberg, Phys. Rev. A **20**, 194 (1979)
20. K. Jung, Th. Antoni, R. Muller, K.H. Kochem, H. Ehrhardt, J. Phys. B **15**, 3535 (1982)
21. W. Sun, M.A. Morrison, W.A. Isaacs, W.K. Trail, D.T. Alle, R.J. Gulley, M.J. Brennan, S.J. Buckman, Phys. Rev. A **52**, 1229 (1995)
22. H. Tanaka, T. Yamamoto, T. Okada, J. Phys. B **14**, 2081 (1981)
23. M. Allan, J. Phys. B **38**, 3655 (2005)
24. G.J. Schulz, *Principles of Laser Plasmas*, edited by G. Bekefi (John Wiley, New York, 1976)
25. A.G. Robertson, M.T. Elford, R.W. Crompton, M.A. Morrison, W. Sun, W.K. Trail, Aust. J. Phys. **50**, 441 (1997)
26. B. Schneider, M. Le Dourneuf, Vo Ky Lan, Phys. Rev. Lett. **43**, 1926 (1979)
27. M. Allan, J. Phys. B **18**, 4511 (1985)
28. S.J. Buckman, private communication